Experimental Investigations of Decentralised Control Design for The Stabilisation of Rotor-Gas Bearings

Theisen, Lukas Roy Svane; Galeazzi, Roberto; Niemann, Hans Henrik; Santos, Ilmar

Published in:
Proceedings of the XVII International Symposium on Dynamic Problems of Mechanics

Publication date:
2015

Document Version
Peer reviewed version

DINAME 2015 - Proceedings of the XVII International Symposium on Dynamic Problems of Mechanics
V. Steffen, Jr; D.A. Rade; W.M. Bessa (Editors), ABCM, Natal, RN, Brazil, February 22-27, 2015

Experimental Investigations of Decentralised Control Design for The Stabilisation of Rotor-Gas Bearings

Lukas R. S. Theisen[1], **Roberto Galeazzi**[1], **Henrik Niemann**[1] **and Ilmar F. Santos**[2]

[1]Dept. of Electrical Engineering and [2]Dept. of Mechanical Engineering, Technical University of Denmark, DK 2800 Kgs. Lyngby, Denmark

Abstract: Rotor-gas bearings are attracting increasing interest because of their high speed capabilities, low friction and clean operation. However, hydrostatic rotor-gas bearings show reduced damping characteristics, which makes it challenging to operate the rotating machine at and about the resonance frequencies. Active lubrication of the journal during operations could enhance the damping and stabilisation characteristics of the sytems, and this could be achieved by means of stabilising controllers. This paper investigates the feasibility of using reduced order models obtained through Grey-Box identification for the design of stabilising controllers, capable of enabling the active lubrication of the journal. The root locus analysis shows that two different control solutions are feasible for the dampening of the first two eigenfrequencies of the rotor-gas bearing in the horizontal and vertical directions. Hardening and softening P-lead controllers are designed based on the models experimentally identified, and salient features of both controllers are discussed. Both controllers are implemented and validated on the physical test rig. Experimental results confirm the validity of the proposed approach.

Keywords: Decentralised Control, Rotor-gas Bearings, Damping Injection, Experimental validation

1 INTRODUCTION

Gas bearings are receiving growing attention for their high speed operation capabilities, low friction, and clean and abundant air as lubricant. However, they suffer from low damping and vibration instabilities (Larsen and Santos, 2013; Powell, 1970; Morosi and Santos, 2012; DellaCorte, 2012). The damping and stability properties require enhancement to allow a safe machine operation in presence of disturbances, especially close to the under-damped resonances. A mechatronic approach can provide such enhancement, while at the same time providing robustness and adaptability. The actuation for such a solution can be electromagnetic (Sun et al., 2014), which can be further combined with lubricated bearings (Pizarro Viveros and Nicoletti, 2013) to exploit the beneficial features of both. Other actuations rely on the use of smart materials, e.g. using piezo-ceramics, where the piezo actuators can either be used as pushers on squirrel cages (Palazzolo et al., 1991; Tuma et al., 2013), as pushers on active tilting pads (Qiu et al., 2003) or as servo valves (Morosi and Santos, 2012) controlling the air injection. In the latter approach, the injected air is both a lubricant and it provides the active forces. The controllers for the mentioned systems can either be experimentally tuned (Morosi and Santos, 2012) or based on a model. The design of model based controllers for gas bearings requires models that catch the dynamic behaviour of the journal in the frequency range where control is needed. In Theisen et al. (2014) such a model has been developed exploiting Grey-Box identification techniques for a piezo actuated rotor-gas bearing. Using the fundamental knowledge of rotor-dynamics, a reduced order model was set up and a few key parameters sufficed to describe the dynamics of the bearing for given injection pressure and rotational velocity. Experiments run at a range of different operational conditions in terms of injection pressure and rotational velocity allowed identification of locally valid models of the rotor-gas bearing providing estimates of the unknown parameters, which allowed the formulation of a model valid over the investigated operational range.

This paper investigates the feasibility of using this low complexity model for the design of control systems capable of enhancing the closed-loop damping characteristics by means of active lubrication of the journal. The root locus method is exploited to analyse the spectrum of possible control strategies. Two different control solutions appear to be feasible for the dampening of the first two eigenfrequencies of the rotor-gas bearing in the horizontal and vertical directions. Hardening and softening decentralised P-lead controllers are designed based on the models experimentally identified, and their stabilizing characteristics are analysed both in the frequency and time domain. Both controllers are then implemented and validated on the physical test rig. Experimental results confirm the validity of the proposed approach.

The paper is structured as follows. Section 2 describes the experimental test rig. Section 3 briefly reviews some of the findings about the system modelling presented in Theisen et al. (2014). Section 4 discusses the design of the two decentralized controllers for damping injection, and the respective features are analysed. Section 5 makes a comparative analysis of the numerical and experimental results. Last, some conclusions are drawn in Section 6.

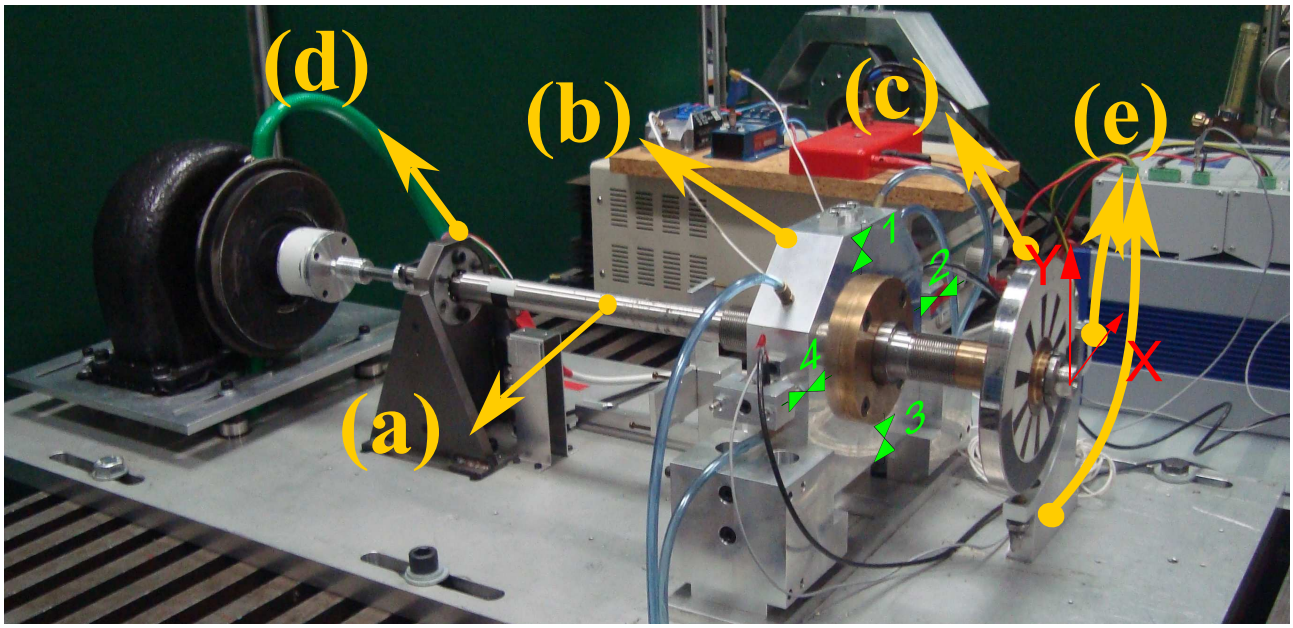

Figure 1: The experimental rotor gas-bearing setup. A flexible shaft (a) is supported by both a ball bearing (d) and the controllable gas bearing (b) with four piezo actuated valves. A disc (c) is mounted on one end to preload the journal and displacement sensors (e) measure the lateral movement of the disc in the shown reference frame.

2 EXPERIMENTAL SETUP OF ROTOR-GAS BEARING TEST RIG

The experimental setup at hand shown in Fig. 1 consists of: a turbine driven flexible shaft (a) supported by both a ball bearing (d) and the controllable gas bearing (b), in which pressurised air is injected through four piezo actuated valves numbered as shown. The manometric injection pressure P_{inj} of the pressurised air is measured by a mechanical gauge before splitting up to the four actuators. The absolute pressure in the valves P_{abs} is assumed to be the sum of the measured pressure and the atmospheric pressure P_{atm}. A disc (c) is mounted on one end to pre-load the journal. The horizontal and vertical shaft deflections $\mathbf{p} \triangleq [p_x, p_y]^{\text{T}}$ are measured at the disc location using eddy current sensors (e) in the coordinate frame specified in the figure. The angular position of the shaft ϕ is measured by an optical encoder. All values are sampled with period $T_s = 0.2ms$.

The position of the i-th valve can be controlled through a voltage input $u_{p,i} \in [0; 10]V$, where an increasing voltage causes the piezo stacks to expand up to $46\mu m$, which closes the valve. The exact expansion varies from stack to stack, and the measured valve positions $y_{p,i}$ are therefore given as voltages $y_{p,i} \in [0; 10]V$, where $0V$ corresponds to an open valve and $10V$ corresponds to a closed valve. Decentralised PD-controllers counteract hysteresis in the valves and control the valve positions, using one commanded valve position $r_x(t)$ for the horizontal valves, and one commanded valve position r_y for the vertical valves. This approach reduces the system from over- to fully actuated. The valves are therefore seen as a "lumped" horizontal valve and a lumped vertical, each having a valve position $[u_x, u_y]^{\text{T}} \triangleq [y_{p,2}(t) - y_{p,4}(t),\ y_{p,1}(t) - y_{p,3}(t)]^{\text{T}}$.

The pressurised air generates a $25\mu m$ thin layer of fluid film in the gap between the shaft and the bearing housing. Given the right conditions of sufficient injection pressure and sufficiently low rotational velocity, the fluid film generates restoring forces and thereby keeps the shaft levitating about a stable equilibrium position. Opening or closing a valve thus perturbs the fluid film. A more thorough description of the setup is available in Morosi and Santos (2012).

3 ROTOR-GAS BEARING MODEL

Theisen et al. (2014) have identified reduced-order models for the rotor-gas bearing through an extensive experimental campaign, where data have been acquired at different injection pressures and rotational velocities. These models have the advantages of being low parametrised and locally well representing the dynamical behaviour of the system. Therefore they appear to be particularly suitable for model-based controller design.

The model is set up as the interconnection of two subsystems: the actuators and the bearing, as shown in Fig. 2. The actuators subsystem models the dynamics of the PD-controlled piezo actuated lumped valves from commanded valve position $\mathbf{r}(t) = [r_x(t), r_y(t)]^{\text{T}}$ to actual valve position $\mathbf{u}(t) = [u_x(t), u_y(t)]^{\text{T}}$. The bearing model is parametrised in shaft rotational speed and injection pressure with input being the actual valve position $\mathbf{u}(t)$ and output being the shaft displacement $\mathbf{p}(t)$. The parameters defining the rotor-gas bearing operational conditions can vary in the following ranges: the rotational speed $\Omega \in [0; 6]\, krpm$, and the injection pressure $P_{\text{inj}} \in [3; 7]\, bar$.

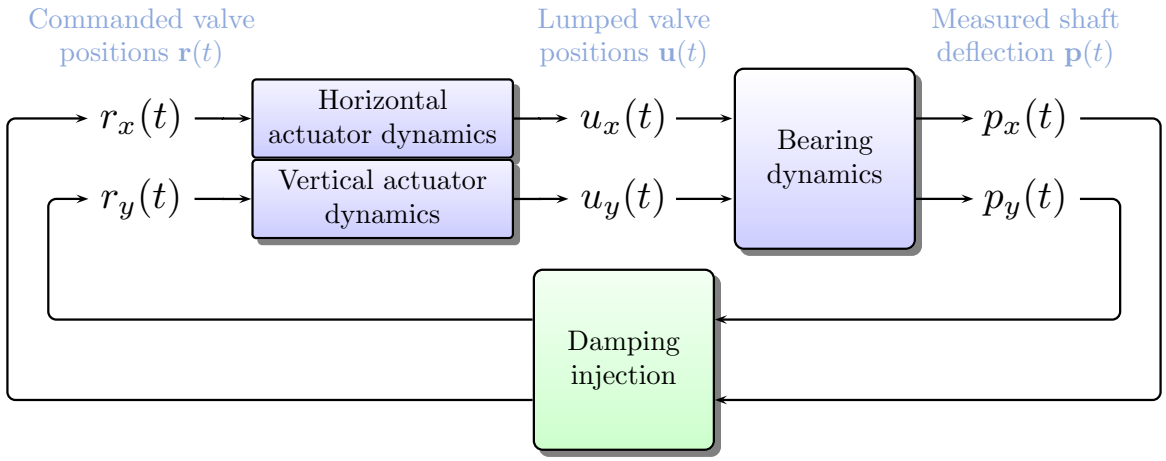

Figure 2: Block diagram of the final system. The horizontal valves are decoupled from the vertical. The measured shaft deflections will be used for feedback controller design generating valve reference positions.

From an input-output perspective the entire model is given by

$$\mathbf{G}_p(s) = \mathbf{G}_{bear}(s)\mathbf{G}_{act}(s), \tag{1}$$

where $\mathbf{G}_{bear}(s)$ is the transfer function matrix from valve position $\mathbf{u}$ to shaft displacement at the disc location $\mathbf{p}$, and $\mathbf{G}_{act}(s)$ is the transfer function matrix from commanded valve position $\mathbf{r}$ to valve position $\mathbf{u}$. The characteristics of the two transfer function matrices will be further discussed in the following sections.

3.1 Modelling of Actuators

The four PD-controlled piezo actuated valves are controlled pairwise, where the two horizontal valves are controlled as one lumped valve, and similarly for the vertical valve. This is described further in Theisen et al. (2014). Each pair of valves are modelled as a second order lowpass filter with two real poles $p_{1,j}$, and $p_{2,j}$ and a stationary gain $\kappa_{a,j}$, where j refers to the horizontal valve x or vertical valve y. The dynamics then reads:

$$\begin{bmatrix} u_x(s) \\ u_y(s) \end{bmatrix} = \underbrace{\begin{bmatrix} G_{a,x}(s) & 0 \\ 0 & G_{a,y}(s) \end{bmatrix}}_{\triangleq \mathbf{G}_{act}(s)} \begin{bmatrix} r_x(s) \\ r_y(s) \end{bmatrix}, \qquad G_{a,j}(s) = \frac{\kappa_{a,j}}{\left(\frac{1}{p_{1,j}}s+1\right)\left(\frac{1}{p_{2,j}}s+1\right)} \tag{2}$$

in which $G_{a,j}(s)$ is the second order filter of the specified form. The poles are located at $p_{1,x} = 3078\ rad/s$,$p_{2,x} = 8143\ rad/s$, $p_{1,y} = 2452\ rad/s$,$p_{1,x} = 6494\ rad/s$. The gains are $\kappa_{a,x} = 1.863\ V/V$, and $\kappa_{a,y} = 1.865 V/V$

3.2 Modelling of Bearing

The combination of flexible shaft and gas bearing can be modelled locally (for constant injection pressure and rotational velocity) as a 2 DOF coupled mass spring damper system combined with an input delay for each valve direction (Theisen et al., 2014). The bearing model input is the actual valve position $\mathbf{u}(s)$ and the output is the shaft displacement $\mathbf{p}(s)$. The model reads:

$$\begin{bmatrix} p_x(s) \\ p_y(s) \end{bmatrix} = \underbrace{\overbrace{\begin{bmatrix} G_{b,xx}(s) & G_{b,xy}(s) \\ G_{b,yx}(s) & G_{b,yy}(s) \end{bmatrix}}^{\triangleq \mathbf{G}_b(s)} \overbrace{\begin{bmatrix} e^{-\tau_x s} & 0 \\ 0 & e^{-\tau_y s} \end{bmatrix}}^{\triangleq \mathbf{G}_\tau(s)}}_{\triangleq \mathbf{G}_{bear}(s)} \begin{bmatrix} u_x(s) \\ u_y(s) \end{bmatrix}, \tag{3}$$

in which $\{G_{b,xx}, G_{b,xy}, G_{b,yx}, G_{b,yy}\}$ are the relevant transfer functions, and the delays model the pressure build-up transients. This is valid over a wide operational range as the model coefficients are parameterised in rotational speed and injection pressure. For constant $\Omega = \bar{\Omega}$ and $P_{\text{inj}} = \bar{P}_{\text{inj}}$, the transfer function can be written with a slight abuse of notation:

$$\mathbf{G}_{bear}(s) = \mathbf{G}_{bear}(\bar{\Omega}, \bar{P}_{\text{inj}}) \tag{4}$$

Choosing more specifically $\bar{P}_{\text{inj}} = 6bar, \bar{\Omega} = 0rpm$, the rotor-gas bearing will have two resonance frequencies ω_x, ω_y. The first $\omega_x = 126.5Hz$ is dominant in the horizontal direction, while the latter $\omega_y = 132.1Hz$ dominates the vertical direction. The corresponding damping factors are $\zeta_x = 0.035$ and $\zeta_y = 0.029$. Figure 3 shows a Bode plot of the

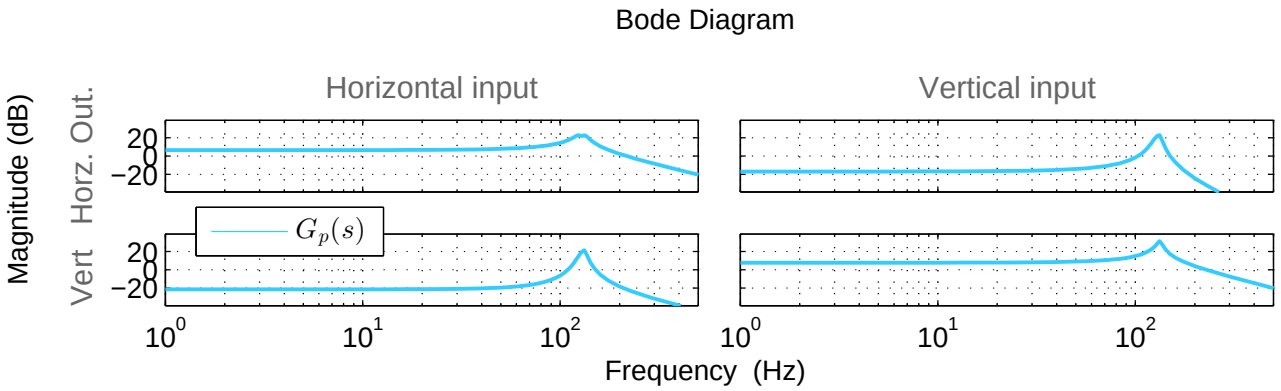

Figure 3: Bode plot of the rotor-gas bearing from commanded valve position to shaft deflection. The system has one clear eigenvalue in each direction, with weaker cross couplings.

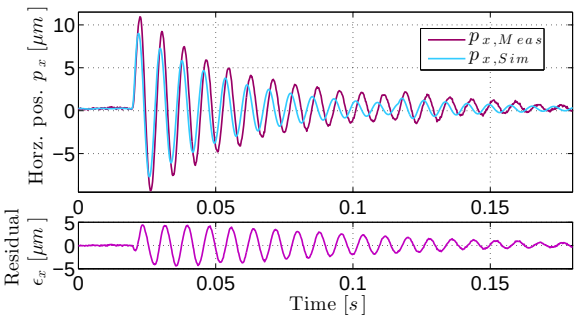

Figure 4: Experimental model validation by horizontal impact response.

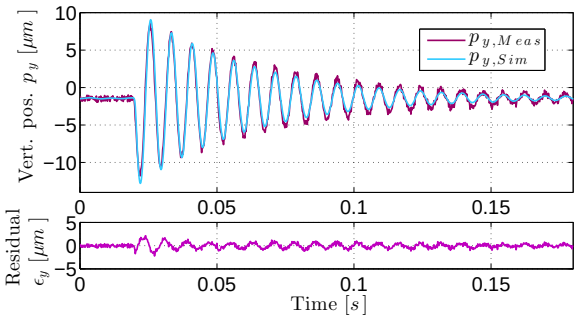

Figure 5: Experimental model validation by vertical impact response.

whole system G_p. The time delays at this operational condition are $\bar{\tau}_x = 0.57ms = 2.8T_s$, $\bar{\tau}_y = 0.123ms = 0.6T_s$. The time delay due to the pressure build-up is approximated using a first order Padé approximation

$$\mathbf{G}_\tau(s) \approx \mathbf{G}_{\tilde{\tau}}(s) \triangleq \begin{bmatrix} G_{\tau,x}(s) & 0 \\ 0 & G_{\tau,y}(s) \end{bmatrix}, \quad G_{\tilde{\tau},j}(s) \triangleq \frac{1 - \frac{\tau_j}{2}s}{1 + \frac{\tau_j}{2}s}, \tag{5}$$

The rotor-gas bearing model then reads

$$\mathbf{p}(s) \triangleq \mathbf{G}(s)\mathbf{r}(s) = \mathbf{G}_b(s)\mathbf{G}_{\tilde{\tau}}(s)\mathbf{G}_{act}(s)\mathbf{r}(s) \tag{6}$$

3.3 Model validation

The bearing model is validated experimentally by impact responses. Application of a horizontal and a vertical impact allows the comparison of the measured and the simulated responses. Figure 4 shows the comparison of the horizontal impact response and Fig. 5 shows the comparison of the vertical impacts. The model deviation is more evident in the horizontal direction resulting in larger residuals defined as the difference between measured and simulated responses $\epsilon_j \triangleq p_{j,meas} - p_{j,sim}$.

4 HARDENING AND SOFTENING DECENTRALISED CONTROL OF ROTOR-GAS BEARING

The reduced damping properties of the rotor-gas bearing can be improved by application of a suitable control strategy.

Problem statement *Given the open loop rotor-gas bearing input-output model* $\mathbf{p}(s) = \mathbf{G}(s)\mathbf{r}(s)$*, with* $\mathbf{p}(s)$ *and* $\mathbf{r}(s)$ *being the Laplace transforms of* $\mathbf{p}(t)$ *and* $\mathbf{r}(t)$*, design a control system that fulfils the following requirements:*

1. *To increase the damping and reject disturbances around the two first eigenfrequencies of the rotor-gas bearing system by at least a factor two while*
2. *using a sufficiently low control effort to avoid actuator wear.*

The rotor-gas bearing model Eq. 6 (Fig. 3) shows that the direct couplings from horizontal valves to horizontal shaft deflection (and similar for the vertical) have gains an order of magnitude larger than the cross coupling gains. This makes decentralised control a feasible option. The controller should improve the damping properties and reject disturbances in a frequency range around the first two eigenfrequencies. This can be achieved through the design of a P-lead controller. The horizontal and vertical P-lead controllers $K_{pl,x}$ and $K_{pl,y}$ thus form the controller $\mathbf{K}_{pl}$, such that:

$$\begin{bmatrix} r_x(s) \\ r_y(s) \end{bmatrix} = -\mathbf{K}_{pl}(s) \begin{bmatrix} p_x(s) \\ p_y(s) \end{bmatrix}, \quad \mathbf{K}_{pl}(s) \triangleq \begin{bmatrix} K_{pl,x}(s) & 0 \\ 0 & K_{pl,y}(s) \end{bmatrix} H_{lp}(s), \quad K_{pl,j}(s) \triangleq \kappa_j \frac{\tau_j s + 1}{\alpha_j \tau_j s + 1}, \tag{7}$$

in which the controller parameters to be tuned are the proportional gain κ_j, the time constant τ_j, and α_j. Each controller contains a lowpass filter $H_{lp}(s)$ to avoid too large high frequency gains. A choice of $H_{lp}(s)$ as a n_s-th order lowpass filter with bandwidth $b_{lp} = 1000Hz$,$n_s = 2$ and unity DC-gain gives sufficient results. The developed model Eq. (6) provides an excellent basis for off-line design, which avoids the risk of instability during on-line tuning. Upon closing the loop using the controller $\mathbf{K}_{pl}$, the output sensitivity $\mathbf{S}_o$ and closed-loop controller activity $\mathbf{K}_{pl}\mathbf{S}_o$ can be calculated:

$$\mathbf{S}_o(s) \triangleq (\mathbf{I}_2 + \mathbf{G}(s)\mathbf{K}_{pl}(s))^{-1} \tag{8}$$

The output sensitivity $\mathbf{S}_o(s)$ and closed-loop controller activity $\mathbf{K}_{pl}\mathbf{S}_o(s)$ are useful tools for tuning the control system's gains, since they provide clear measures of the controller action over the desired range of frequencies. The fulfilment of requirement 1) implies that the output sensitivity close to the resonance frequencies ω_j satisfies $|S_o(\omega_j)| < 0.5$. Further, to avoid simply shifting the resonance, the peak should be sufficiently low, here chosen as $||S_o||_\infty \leq 1.6$. At lower and higher frequencies control effort is not desired.

The specifications can be achieved through two designs, which differ in the sign of proportional action. The natural approach is to establish a negative feedback control law, which implies that the sign of the proportional gain in Eq. (7) is positive, $\kappa_j > 0$. This is what we address as the *hardening decentralised controller*. An alternative approach, which still achieves the control objectives, is to establish a positive feedback by means of a negative proportional action, $\kappa_j < 0$. This is what we address as the *softening decentralised controller*.

The controller must satisfy the Bode sensitivity integral (Freudenberg and Looze, 1985), which states that the sensitivity function $S(s)$ evaluated at $s = j\omega$ satisfies the following integral constraint $\int_0^\infty \ln |S(j\omega)|\, d\omega = 0$ which implies that any linear control law that reduces the sensitivity function in an interval must increase the sensitivity function in some other interval. Moreover, the presence of the time delays, modelled as first order non-minimum phase system, sets limitations on the achievable performance due to the interpolation constraints (Skogestad and Postlethwaite, 2005): denote the right half plane zeros $z_m, m \in \{1, ..., M\}$. The sensitivity must then satisfy $S(z_m) = 1$.

A *hardening decentralized controller* places the sensitivity peak at the closed-loop eigenfrequency, which is higher than the open loop eigenfrequency. On the other hand,the *softening decentralized controller* places the sensitivity peak at a lower frequency. In this aspect, the time delay in the bearing dynamics plays an important role as it sets an upper bandwidth limit: using the hardening control approach it is not possible to achieve a sufficient reduction in sensitivity at the resonance frequency without it being at the cost of an unacceptably high sensitivity peak at higher frequencies. However, this is achievable using softening control. Evaluation of the sensitivity functions obtained through the *hardening decentralized controller* and the *softening decentralized controller* clearly confirm the analysis, and experimental results verify the sensitivity functions.

4.1 Controller Designs

The choice of gains for the controllers is no trivial task. Figure 6 shows a root locus for the horizontal direction using only proportional gain κ_x. The gain must be within $\kappa_x \in [-0.47; 0.05]$ to avoid instability. For the hardening case, the controller soon destabilises the rotor-gas bearing, whereas for the softening case, proportional action alone is enough to achieve an increase in stabilisation. This is reflected in the choice of controller gains. The hardening and the softening controllers' parameters are listed in Table 1, and the respective Bode diagrams are shown in Fig. 7. The lead action in the hardening case improves the damping characteristics, whereas for the softening controller the derivative action is minimal, and could in practice be neglected. Further, the root locus shows that positive proportional control can move the system eigenvalues to the real axis, thereby achieving a damping factor of 1. Experimental results validating this are available in Theisen et al. (2014). Such a design however violates the sensitivity requirement $||S_o||_\infty \leq 1.6$ and is therefore not considered further here. The output sensitivities shown in Fig. 8 validate that both designs achieve the specified sensitivity requirements.

For many applications controllers are used to provide sufficient damping to allow safe crossing of critical speeds. The main disturbance from mass unbalance thus increases in frequency. Using the hardening controller design, these oscillations are attenuated at low frequencies, but are then amplified (compared to open loop) when the rotational speed becomes supercritical. This is avoided by the softening design, where the sensitivity reduces before the critical speed and remains low even in supercritical operation.

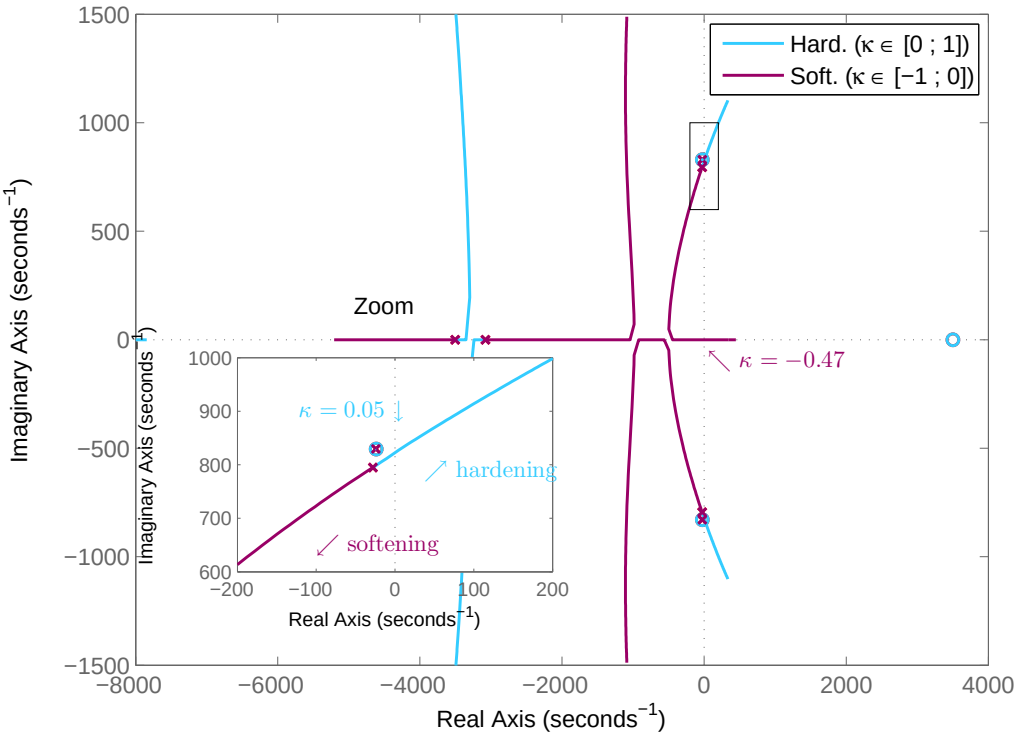

Figure 6: Root locus for the horizontal direction using only proportional gain $\kappa \in [-1; 1]$.

Table 1: Controller parameters for controller of form Eq. (7)

Design	Gain κ_x $[V/\mu m]$	Gain κ_y $[V/\mu m]$	Time Const. τ_x $[ms]$	Time Const. τ_y $[ms]$	Alpha α_x $[-]$	Alpha α_y $[-]$
Hardening	0.0061	0.0133	20.8	11.3	0.0036	0.0148
Softening	-0.132	-0.090	0.30	0.0200	0.0077	0.0077

5 EXPERIMENTAL AND NUMERICAL VALIDATION

This section presents validation of the controller designs. Both designs have been validated experimentally and numerically in the non-rotating case, and numerically for the vertical direction with a rotational speed of $\bar{\Omega} = 4.0krpm$.

5.1 Experimental and Numerical Validation - Non-Rotating Case

Both controllers have been discretised and implemented on the rotor-gas bearing system. Impact responses were collected both for the open and closed-loop bearing for both the horizontal (shown in Fig. 10) and rhe vertical direction (shown in Fig. 9). In both impact directions the softening controller achieves a clear damping increase. The hardening controller however only achieves a damping increase in the vertical direction. The unsatisfactory performance may well stem from the model discrepancies found in the horizontal open loop model validation. Figure 11 shows individual comparisons between the measured and the simulated impact responses, where the model is simulated using the same impact force. The responses validate that the obtained performances are close to the predicted in all cases other than the horizontal hardening impact response. The revealed model deviation should be investigated further.

5.2 Numerical Validation - Rotating Case

The designed controllers have been tested in a rotating case as well by simulating impacts on the open-loop and closed-loop system with a rotational speed $\bar{\Omega} = 4.0\ krpm$. Figures 12 and 13 show simulated horizontal and vertical impact responses in 1) open loop and using 2) the hardening and 3) the softening controller design. Both controllers increase the damping compared to the open loop case with satisfactory performance. The modified dynamics due to the rotation however benefits the hardening controller most in the vertical case, where it performs slightly better than the softening one. Closed-loop experimental results for rotating conditions are available in Theisen et al. (2014).

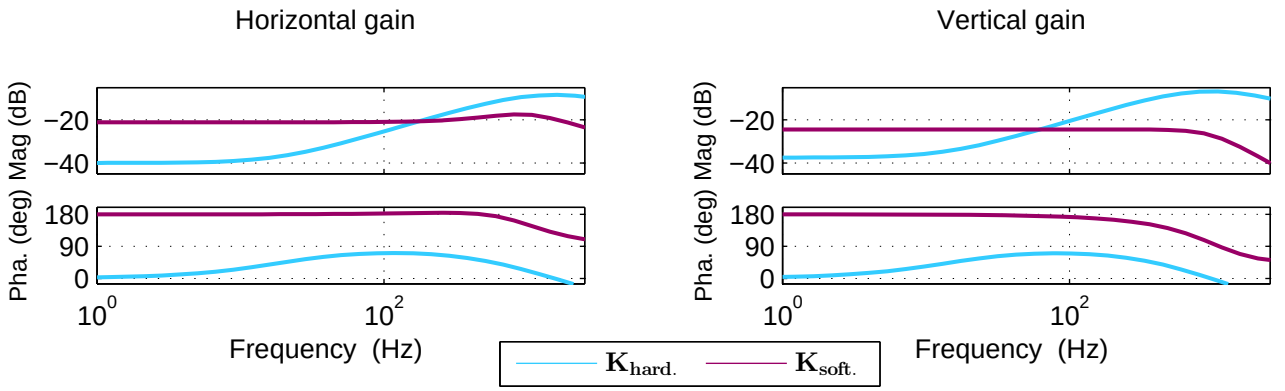

Figure 7: Comparison of controller gains for the hardening and softening designs. left) $K_{Pl,x}(s)$, right) $K_{Pl,y}(s)$. Note the phase difference between the hardening and softening designs.

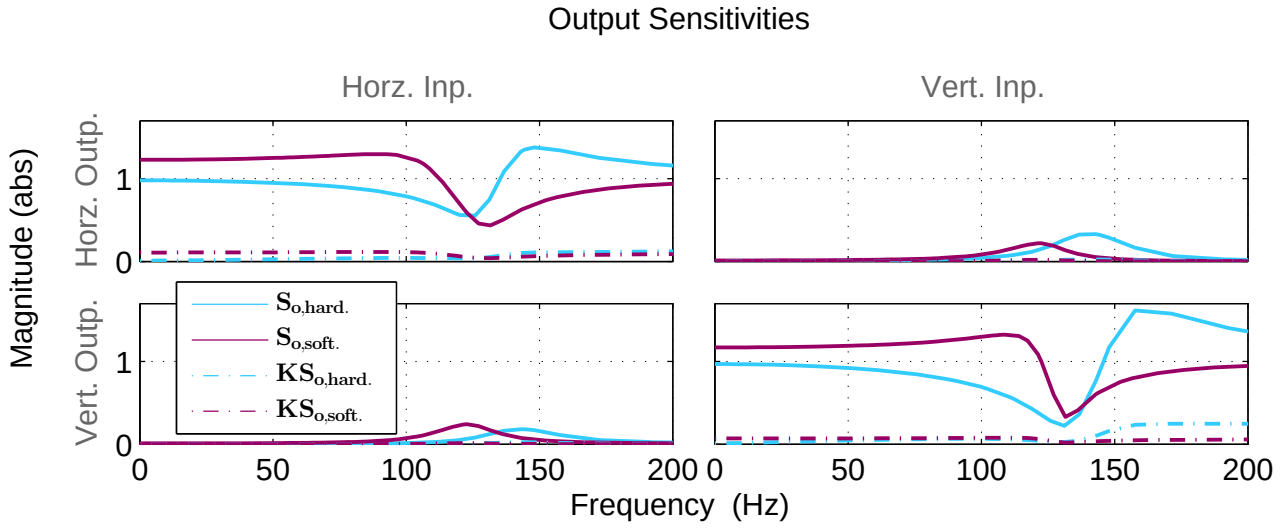

Figure 8: Comparison of output sensitivities using the hardening and softening designs. The hardening design already achieves some performance for low rotational speeds ($|\mathbf{S}_{0,hard.}(0)|< 1$), whereas the softening amplifies disturbances at low frequencies ($|\mathbf{S}_{0,soft.}(0)|> 1$). Both controllers have decently small controller activities $\mathbf{KS}_o$

6 CONCLUSION

High-speed rotating machines with flexible shaft and gas bearings are complex systems, whose dynamics is generally modelled by means of partial differential equations naturally arising from the physics governing the system behaviour. Those models are not suitable for the design of control systems, which are instead preferably based on low order models that capture the essential dynamics in focus of the control objectives.

This paper has successfully investigated the feasibility of designing a control system for the stabilisation of a rotor-gas bearing based on a 2 degrees-of-freedom mass-spring-damper equivalent model, previously identified in Theisen et al. (2014). Application of the root locus method pointed out the possibility of designing two types of decentralised P-lead controllers, one determining a hardening of the closed-loop system, and one achieving a softening of the closed-loop system. Both controllers fulfil the control objectives. However, the decentralised softening controller showed better performance than the hardening one in terms of damping injection in both the horizontal and vertical directions.

The designed controllers have been successfully implemented and tested on the physical rotor-gas bearing test rig. The experimental results available for the non-rotating case are in very good agreement with the numerical simulations, especially for the softening controller. Numerical results validate damping enhancement for rotating conditions as well. This clearly confirms the feasibility of designing stabilising controllers for the rotor-gas bearing exploiting low complexity models obtained through system identification techniques.

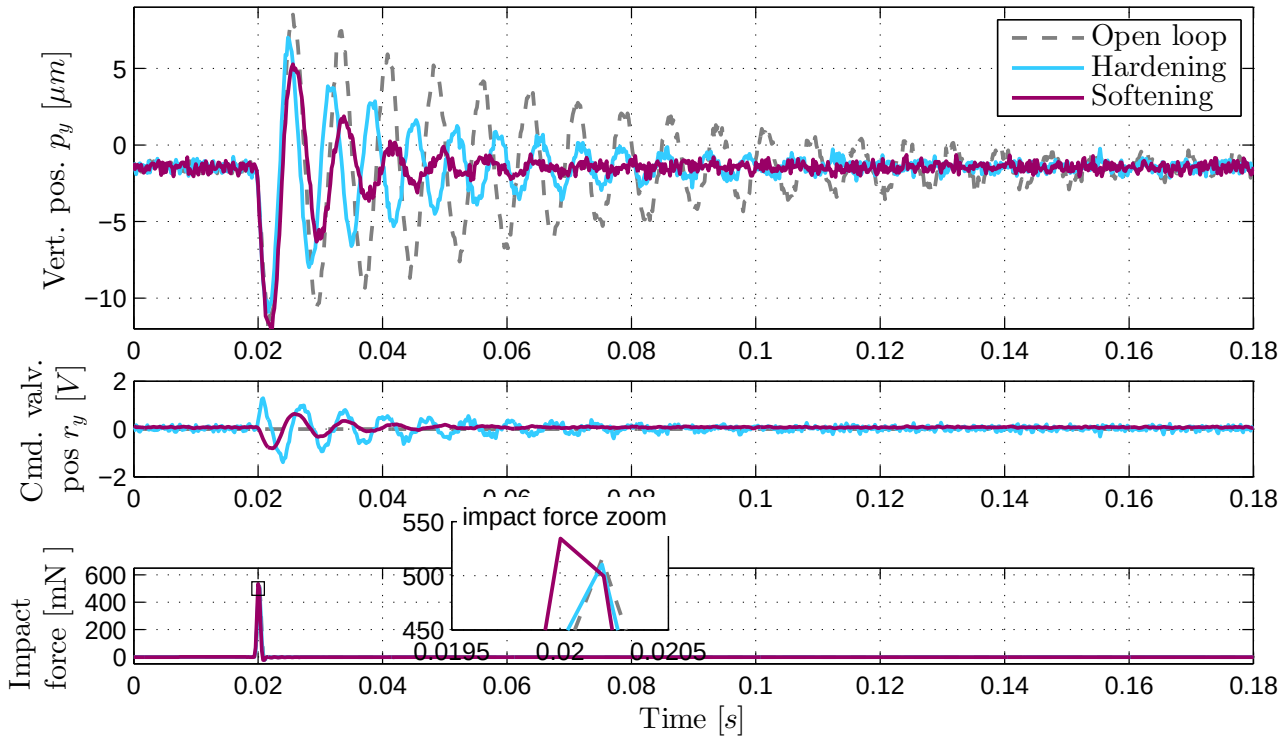

Figure 9: Experimental comparison of vertical impact responses for cases: 1) without control, 2) using hardening, 3) using softening design.

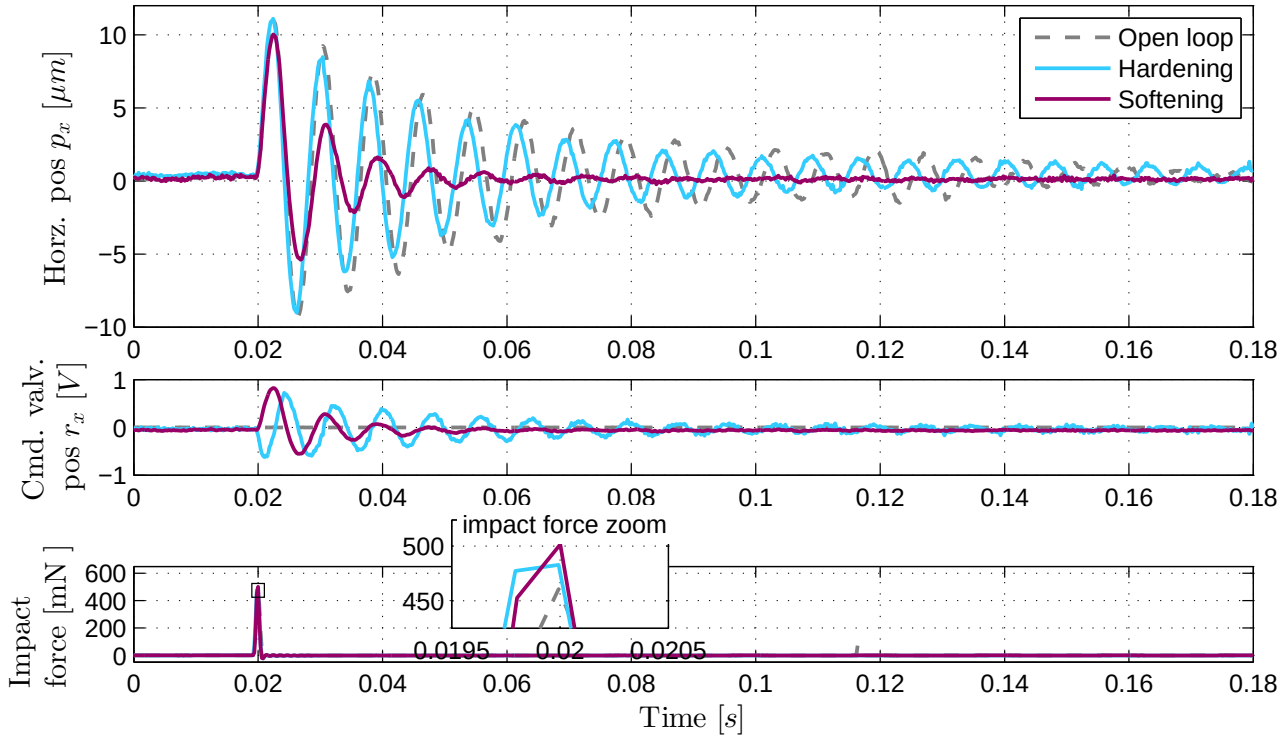

Figure 10: Experimental comparison of horizontal impact responses for cases: 1) without control, 2) using hardening, 3) using softening design.

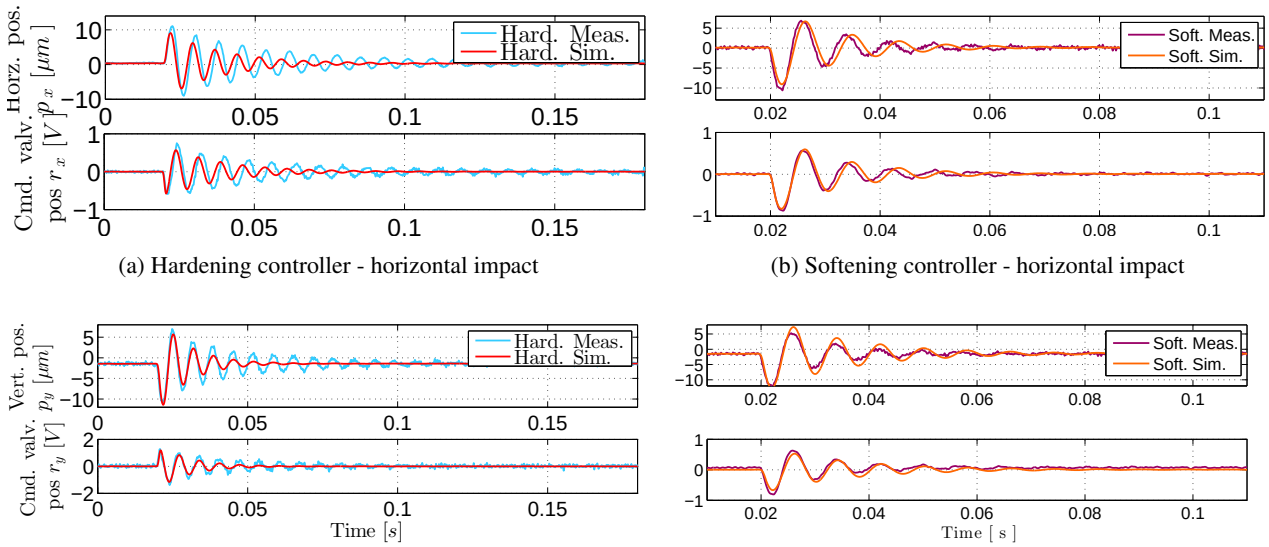

(a) Hardening controller - horizontal impact

(b) Softening controller - horizontal impact

(c) Hardening controller - vertical impact

(d) Softening controller - vertical impact

Figure 11: Experimental validation of controller designs by impact responses: measured impact vs simulated using the coresponding measured impacts from Fig. 9.

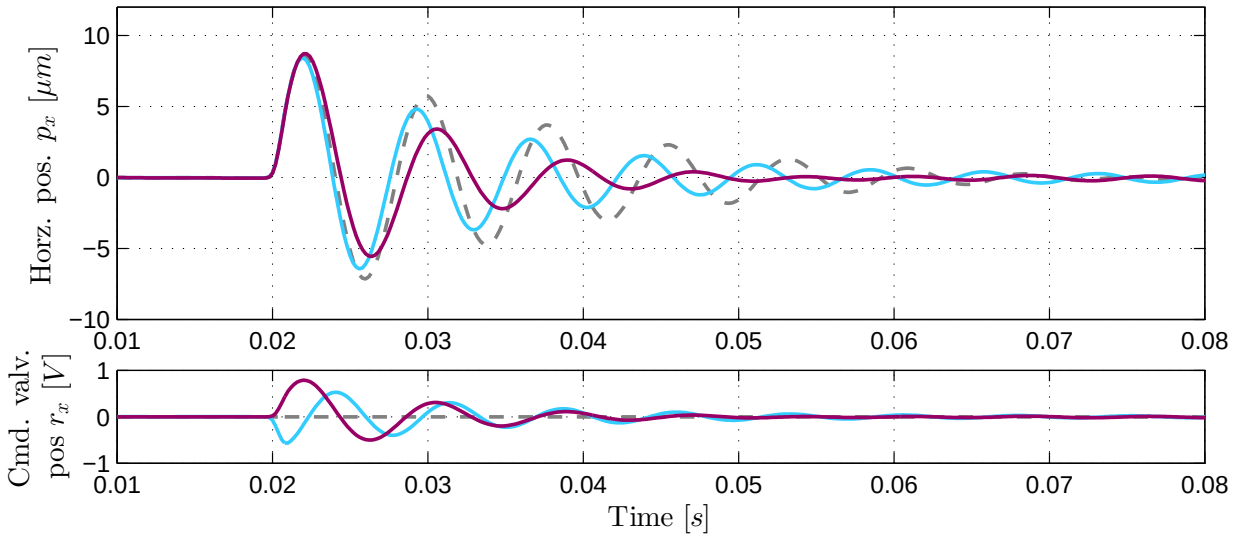

Figure 12: Numerical validation for horizontal impact response at $\bar{\Omega} = 4.0\ krpm$ for cases: 1) without control, 2) using hardening, 3) using softening design.

ACKNOWLEDGMENTS

The Danish Ministry of Science, Innovation and Higher Education is gratefully acknowledged for the support to the FTP research project 12-127502.

REFERENCES

DellaCorte, C. (2012). Oil-free shaft support system rotordynamics: Past, present and future challenges and opportunities. *Mechanical Systems and Signal Processing*, 29(0):67 – 76.

Freudenberg and Looze (1985). Right half plane poles and zeros and design tradeoffs in feedback systems. *IEEE Transactions on Automatic Control*, 30(6):555–565.

Larsen, J. S. and Santos, I. F. (2013). Compliant foil journal bearings-investigation of dynamic properties. *SIRM 2013*.

Morosi, S. and Santos, I. F. (2012). Experimental investigations of active air bearings. In *ASME Turbo Expo 2012: Turbine Technical Conference and Exposition*. American Society of Mechanical Engineers.

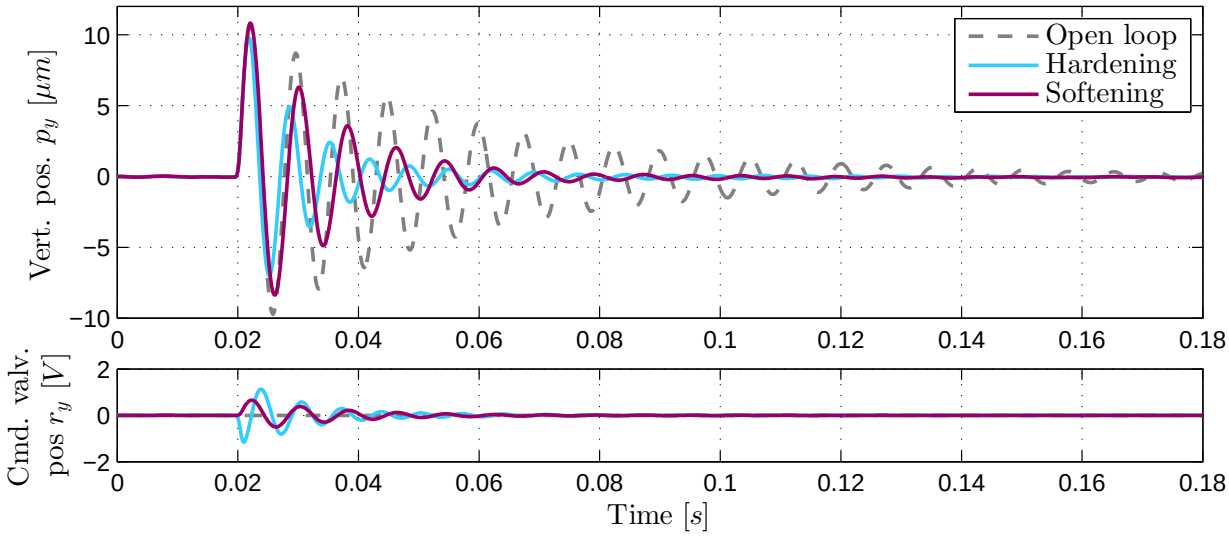

Figure 13: Numerical validation for vertical impact response at $\bar{\Omega} = 4.0\ krpm$ for cases: 1) without control, 2) using hardening, 3) using softening design.

Palazzolo, A., Lin, R., Alexander, R., Kascak, A., and Montague, J. (1991). Test and theory for piezoelectric actuator-active vibration control of rotating machinery. *Journal of vibration, acoustics, stress, and reliability in design*, 113(2):167–175.

Pizarro Viveros, H. and Nicoletti, R. (2013). Lateral Vibration Attenuation of Shafts Supported by Tilting-Pad Journal Bearing With Embedded Electromagnetic Actuators. *Journal of Engineering for Gas Turbines and Power*, 136(4):042503.

Powell, J. W. (1970). A review of progress in gas lubrication. *Review of Physics in Technology*, 1(2):96.

Qiu, J., Tani, J., and Kwon, T. (2003). Control of Self-Excited Vibration of a Rotor System With Active Gas Bearings. *Journal of Vibration and Acoustics*, 125(3):328.

Skogestad, S. and Postlethwaite, I. (2005). *Multivariable Feedback Control: Analysis and Design*. John Wiley & Sons.

Sun, Z., He, Y., Zhao, J., Shi, Z., Zhao, L., and Yu, S. (2014). Identification of active magnetic bearing system with a flexible rotor. *Mechanical Systems and Signal Processing*, 49(1-2):302–316.

Theisen, L. R. S., Niemann, H., Santos, I. F., Blanke, M., and Galeazzi, R. (2014). Modelling and identification for control of rotor gas bearings. *Submitted to Mechanical Systems and Signal Processing*.

Tuma, J., Simek, J., Skuta, J., and Los, J. (2013). Active vibrations control of journal bearings with the use of piezoactuators. *Mechanical Systems and Signal Processing*, 36(2):618–629.